Available online at www.sciencedirect.com

ScienceDirect

www.elsevier.com/locate/jes

JES JOURNAL OF ENVIRONMENTAL SCIENCES

www.jesc.ac.cn

Pollutants identification of ambient aerosols by two types of aerosol mass spectrometers over southeast coastal area, China

Jinpei Yan[1,*], *Liqi Chen*[1], *Qi Lin*[1], *Shuhui Zhao*[1], *Lei Li*[2]

1. *Key Laboratory of Global Change and Marine-Atmospheric Chemistry, Third Institute of Oceanography, SOA, Xiamen 361005, China*
2. *Institute of Atmospheric Environment Safety and Pollution Control, Jinan University, Guangzhou 510632, China*

ARTICLE INFO

Article history:
Received 15 February 2017
Revised 15 May 2017
Accepted 23 June 2017
Available online 1 July 2017

Keywords:
Aerosol
Size distribution
Chemical composition
Aerosol mass spectrometer
Aerosol source

ABSTRACT

Two different aerosol mass spectrometers, Aerodyne Aerosol Mass Spectrometer (AMS) and Single Particle Aerosol Mass Spectrometer (SPAMS) were deployed to identify the aerosol pollutants over Xiamen, representing the coastal urban area. Five obvious processes were classified during the whole observation period. Organics and sulfate were the dominant components in ambient aerosols over Xiamen. Most of the particles were in the size range of 0.2–1.0 μm, accounting for over 97% of the total particles measured by both instruments. Organics, as well as sulfate, measured by AMS were in good correlation with measured by SPAMS. However, high concentration of NH_4^+ was obtained by AMS, while extremely low value of NH_4^+ was detected by SPAMS. Contrarily, high particle number counts of NO_3^- and Cl^- were given by SPAMS while low concentrations of NO_3^- and Cl^- were measured by AMS. The variations of POA and SOA obtained from SPAMS during event 1 and event 2 were in accordance with the analysis of HOA and OOA given by AMS, suggesting that both of AMS and SPAMS can well identify the organic clusters of aerosol particles. Overestimate or underestimate of the aerosol sources and acidity would be present in some circumstances when the measurement results were used to analyze the aerosol properties, because of the detection loss of some species for both instruments.

Introduction

Particulate matter (PM) has become the primary pollutants in urban areas, since large quantities of aerosol particles were inevitably emitted into atmosphere with the rapid development of economic and energy consumptions (Yan et al., 2016; Yang et al., 2010). The importance of aerosols has received considerable attention throughout the world because of their impacts on air quality, human health (Buonanno et al., 2013; Brook et al., 2002), atmospheric visibility (Kanakidou et al., 2005) and global climate change (Prather, 2009; Alfarra et al., 2004). Different aerosol particle compositions would cause different health risks (Kang et al., 2004; Kim et al., 2008) and was also necessary to identify their sources and predict their effects on atmospheric processes.

Xiamen island located in the Southeast China is a well-known tourism coastal city on the Southeast coast of China and one of the Cleanest Cities of China (http://www.cnemc.cn/) with a sub-tropical climate under the influence of the Asian monsoon. In cold seasons of winter and spring, a northeasterly wind becomes the most prevailing wind direction. Air masses mainly come from northern China during wintertime. While in summertime, air masses from marine affect the local atmospheric quality. Therefore, aerosol particles in Xiamen area are not only related to anthropogenic activities, such as vehicular, coal combustion, and ship and industrial emissions,

* *Corresponding author*. E-mail: jpyan@tio.org.cn (Jinpei Yan).

http://dx.doi.org/10.1016/j.jes.2017.06.030
1001-0742/

but also affected by the marine sources, such as sea salt particles, and sulfate and biological aerosols (Zhao et al., 2011; Yan et al., 2015; Zhang et al., 2011, 2012). In urbanized coastal zone, anthropogenic nitric acid reacts with sea salt to form coarse particles of sodium nitrate ($NaNO_3$), which increases the deposition velocities of particles and cleanses the atmosphere of acidic gaseous aerosol precursors. Moreover, the surface reaction often occurs between sulfuric acid and sodium chloride, producing sodium sulfate (Falkowska and Lewandowska, 2004; Chalbot et al., 2013). The biological components are primarily emitted into the atmosphere through a bubble bursting mechanism, usually as a part of mixed aerosol composed of other organic and inorganic compounds (Aller et al., 2005; Després et al., 2012; O'Dowd et al., 2004). In coastal area, the interaction between marine aerosols and anthropogenic particles was rather complicated and ambiguous. Therefore, it is important to investigate the chemical and physical properties of aerosol particles to identify their potential sources, formation mechanisms and atmospheric processes.

Recently, studies on aerosol properties over the coastal area of Xiamen including size distribution, source identification (Zhao et al., 2011; Zhang et al., 2012) have been present. However, offline filter sampling methods were conducted in previous studies with low time resolution. Long sampling time, 24 hr or even longer, was required to reach detection limits for offline filter analysis (Zhang et al., 2007). Since the physico-chemical process of aerosol particles in atmosphere occurred every moment, the physical and chemical characteristics of aerosol changed rapidly within a short time. Offline filter sampling methods were difficult to probe into the physico-chemical processes of aerosol particles in some special atmospheric events, because of a long sampling and analysis time. Therefore, high-time-resolution measurement was important and necessary to study the quick change of aerosol sources and compositions in ambient atmosphere.

Since online aerosol mass spectrometry was able to provide size and chemical information of aerosol particles in atmospheric environment with high-time-resolution (Sullivan et al., 2007; Spencer et al., 2007), It was used to characterize the aerosol chemical compositions, aerosol sources, mixed state and secondary aerosol formations, *etc.* In recent years, two types of aerosol mass spectrometers were used in atmospheric aerosol investigation, such as aerosol time-of-flight mass spectrometer (ATOFMS, Dall'Osto and Harrison, 2006; Dall'Osto and Harrison, 2012; Steve et al., 2012), and quadrupole aerosol mass spectrometer (Q-AMS, Jayne et al., 2000; Jimenez et al., 2003; Alfarra et al., 2004; Sun et al., 2010). Recently, a newly developed single particle mass spectrometer (SPAMS) was widely used in ambient aerosol researches (Li et al., 2014; Ma et al., 2016), which was able to provide the size and chemical information of a single particle which was important to identify aerosol sources. SPAMS and AMS have been extensively applied in atmospheric aerosol investigation. However, the comparisons of measurement results obtained by both instruments have not been elucidated. Different measurement results would be present when different types of measurement instruments were used to identify aerosol pollutants. This study aims to provide detailed comparisons of physical–chemical properties of atmospheric aerosol particles measured by SPAMS and AMS and understand impacts of measurement instruments on the atmospheric aerosol sources and pollutant identification. In this case, the investigation of aerosol pollutants over the coastal urban zone Xiamen, China was carried out using SPAMS and AMS simultaneously to demonstrate the discrepancy in aerosol measuring results.

1. Methods and data

1.1. Sampling site

The observation site (24°16′N, 118°05′E) was located on the platform of 10th Research Building about 45 m height above the sea level. This site is located in the seaside of southern Xiamen city, which represents the coastal urban district due to the impact of traffic, sea salt, residential, construction, ship and coal-fired emissions.

1.2. Instruments and measurements

The observation system included the sampling, control and measurement instruments. A $PM_{2.5}$ sampling cyclone (URG Corp., USA) was set to conduct intensive measurements. A Quadruple Aerosol Mass Spectrometer (AMS, Aerodyne Research Inc., USA) and a single particle mass spectrometry (SPAMS 0515, Guangzhou Hexin Analytical Instrument Co., Ltd., Guangzhou, China) were deployed to analyze the size-resolved chemical composition of aerosol particles simultaneously. A $PM_{2.5}$ sampler (MS310, USA) was employed at the same time to collect $PM_{2.5}$ samples at every 24 hr during the observation period. Particulates were collected on quartz fiber filters (Whatman, UK). Samples were stored in refrigerator at −20°C after sampling for later analysis. Eight samples were obtained during the observation period. Meteorological parameters were monitored by a weather transmitter WXT520 (Vaisala Co., Ltd., Finland).

1.3. Water-soluble inorganic ions analysis

A quarter of each blank and sample quartz fiber filter were cut into fine strips and dipped into 10 mL ultrapure water (18.2 MΩ/cm), and water-soluble inorganic ions from the samples were extracted by ultrasonic bath for 30 min. The extract solutions were filtered with a Polytetrafluoroethylene (PTFE) syringe filters (Pall Co., Ltd., USA). An ion chromatography system (ICs-2500, Dionex, USA) was used to determine the concentration of aerosol water-soluble ions. Field blank value was subtracted from the sample concentrations.

1.4. AMS and data analysis

Aerodyne Aerosol Mass Spectrometer (AMS) operation principles have been described in detail by Jayne et al. (2000) and Jimenez et al. (2003). In this study, the AMS was alternated between two modes, the mass spectrum (MS) mode and particle time-of-flight (PTOF) mode. The PTOF mode was a size distribution measurement mode for selected *m/z* settings of the AMS (Jimenez et al., 2003; Allan et al., 2003). The PTOF mode operation, signals of eleven *m/z*'s representative of NO_3^-

(*m*/z 30 and 46), SO_4^{2-} (*m*/z 48, *m*/z 64 and 81, *m*/z 82, *m*/z 98), organics (*m*/z 43, 44, 55, and 57), NH_4^+ (*m*/z 16), H_2O (*m*/z 18), and N_2 (*m*/z 28) were recorded as a function of particle size. Mass concentration of each species was determined by summing up ion signals in the corresponding partial spectra using the fragmentation table approach described in Allan et al. (2003). In this study, the average IE value (=1.96e−6) and default relative ionization efficiency (RIE) values (1.15 for sulfate, 1.10 for nitrate, 1.30 for chloride, 1.40 for organics and 2.00 for water) were used to determine the conversion of measured AMS ion intensities to mass concentrations (Yan et al., 2015). The RIE (=4.3) for ammonium was determined based on the analysis of pure ammonium nitrate particles. Constant collection efficiency (CE) of 0.5 was used to calculate mass concentrations from AMS mass spectra. Previous field studies have shown that a constant value (CE = 0.5) was used for ambient aerosol quantification and present good agreements of measurements between AMS and collocated instruments (Drewnick et al., 2004; Sun et al., 2010).

The signal from ambient aerosol was determined by subtracting the background signal from the total signal. The detection limits were defined as three times the standard deviation of the corresponding species signal in the filtered air. The integration time employed for this study was 30 min.

1.5. SPAMS and data analysis

The detection method of fine particle used Single Particle Aerosol Mass Spectrometer (SPAMS) was described in detail by Li et al. (2011). Particles are introduced into the vacuum system through a critical orifice, then focused and accelerated to specific velocities. The particle beam passes through two continuous diode Nd:YAG lasers (532 nm), where the scattered light is detected by two Photomultiplier Tube (PMT). The velocity of a single particle is determined and converted into its aerodynamic diameter. Individual particle is ionized by a 266 nm Nd:YAG laser to produce positive and negative ions. The fragments are analyzed by a bipolar time-of-flight mass spectrometer. The vacuum aerodynamic diameter can be obtained using a calibration curve created from the measured velocities of series of polystyrene latex spheres (Nanosphere Size Standards, Duke Scientific Corp., Palo Alto) with defined sizes. The power density of ionization laser was kept at 1.56×10^8 w/cm^2.

The particle size and mass spectra information were analyzed using YAADA software toolkit (http://www.yaada.org/) (Allen, 2005). An adaptive resonance theory based neural network algorithm (ART-2a) was applied to cluster individual particle into separate groups based on the presence and intensity of ion peaks in single particle MS (Song et al., 1999), with a vigilance factor of 0.65, learning rate of 0.05, and a maximum of 20 iterations.

2. Results and discussions

2.1. Meteorological parameters and atmospheric processes

A continuous observation was carried out from 9th to 21st September, 2013. The meteorological parameters, chemical compositions obtained by SPAMS and AMS are illustrated in Fig. 1. The dominant wind directions were northeasterly during the sampling period except during event 2 in Xiamen. In this study, a total of 2,082,600 particles were sized and approximately 627,810 individual particles with both positive and negative ion mass spectra were collected by SPAMS.

Real-time aerosol chemical concentrations can provide a useful clue to track the atmospheric processes. Two types of aerosol mass spectrometers were used to monitor the aerosol chemical compositions in real-time. Since AMS can only detect the volatile and semi-volatile components (such as SO_4^{2-}, NO_3^-, NH_4^+, Cl^- and organics), the mass concentrations of those aerosol species were employed to characterize the implicit nature of atmospheric events. As marked in Fig. 1, there were five obvious processes during the observation period according to the variations of the aerosol species and concentrations. As seen in Fig. 1b and c, the aerosol chemical compositions during event 1, event 3 and event 5 were very similar, representing the general aerosol pollutant characteristics over the coastal area in Xiamen. Organics and sulfate were the major aerosol components and the organic concentration was higher than sulfate in those events. Additionally, the dominant hourly wind directions were northeast in Xiamen during event 1, event 3 and event 5. Hence, the three events can be classified as the same atmospheric case (we abbreviated the three events as event 1 in the following discussions). However, during event 2, organics were the only dominant components, accounting for more than 50% and 75% with SPAMS and AMS measurement individually during this period. Generally, organic species was used to investigate the contributions of different emission sources of fossil combustion, such as traffic exhaust, biomass burning and coal combustion. (Yin et al., 2012). As seen in Fig. 1a, the wind patterns switched from northeasterly during event 1 to northwesterly during event 2. Note that the regions to the northwest of the sampling site are manufacturing districts. Large emission sources of fossil combustion and other industry air pollutants were located to the northwest of the sampling site, while regions to the northeast of the sampling site had relatively few industry sources (Yan et al., 2015). Since the sampling site was located extremely close to the manufacturing districts (<10 km), pollutant emissions from this region can directly affect the air quality in the sampling site if the air masses were derived from the manufacturing districts. Consequently, variations of aerosol chemical species during event 2 were likely associated with the emission from manufacturing districts in this study. Relative low wind speed was present during event 2, which contributed the accumulation of pollutants due to poor diffusion conditions.

By contrast, the concentration of sulfate was the primary component in the aerosols, exceeding the organic concentration during event 4. Comparing to during event 1 and event 2, the percentage of organics, NO_3^- and Cl^- were lower during event 4, which accounted for 28.85%, 14.91% and 12.07%, respectively (Fig. 1b), while the concentration of NH_4^+ in event 4 was higher than during event 1 and event 2. SO_4^{2-}, NO_3^-, and NH_4^+ were believed to originate mainly from secondary pollution particles produced by the transformation of their precursors of SO_2, NO_2 and NH_3 (Wang et al., 2006). Note that the wind direction and wind speed did not make much

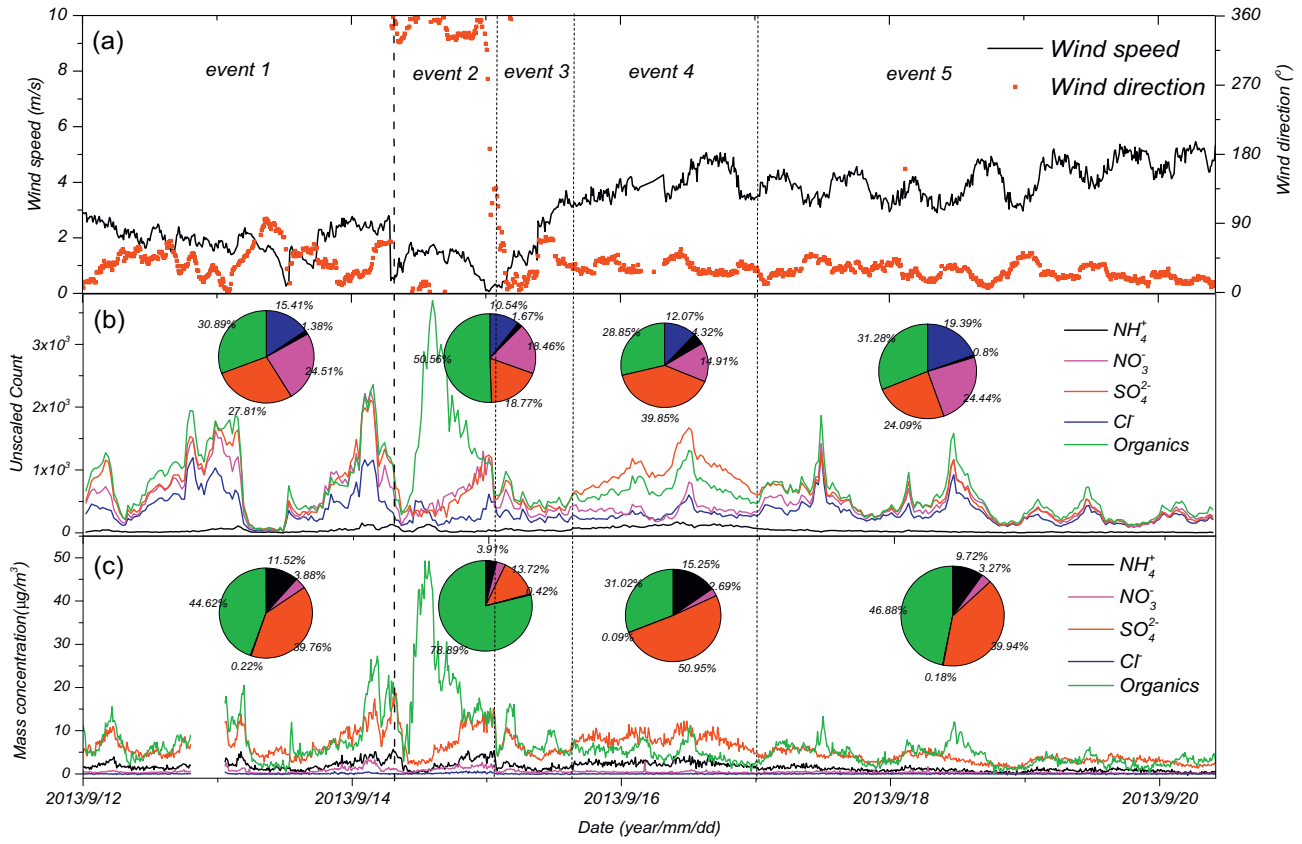

Fig. 1 – Time series (Beijing time) of the meteorological parameters, SPAMS detected particles and the aerosol chemical compositions measured by AMS during September 12 to 21, 2013 in Xiamen. (a) Wind speed and direction; (b) particle number of sulfate, nitrate, ammonium, organics and chloride detected by SPAMS every 30 min; (c) mass concentrations of sulfate, nitrate, ammonium, organics and chloride measured by AMS.

difference between event 4 and event 1. Hence, event 4 can be classified as the secondary inorganic pollution.

2.2. Pollutants identification by AMS and SPAMS

It is useful to found that variation trend of aerosol components time series measured by SPAMS was similar with the variation trend given by AMS, indicating that both instruments can well describe changes of ambient aerosols. Organics and sulfate were the dominant aerosol components for both instruments, accounting for 30.89% and 27.81% individually measured by SPAMS, while the value was about 44.62% and 39.76% given by AMS during event 1. But the measurement result of NO_3^-, Cl^- and NH_4^+ species with AMS and SPAMS was quite different. High value of Cl^- and NO_3^- particle number count was detected by SPAMS, while the concentration of Cl^- and NO_3^- was extremely low with the AMS measurement. Contrarily, high concentration of NH_4^+ was measured by AMS, while very low particle number count of NH_4^+ was detected by SPAMS. During event 1, Cl^-, NO_3^- and NH_4^+ accounted for about 15.41%, 24.51% and 1.38% respectively for the SPAMS measurement, but the value was 0.22%, 1.38% and 11.52% individually for AMS analysis in this study. Similar results were present during the whole observation periods. Fig. 2 shows the correlation of AMS mass concentration and SPAMS particle number count during the whole observation period. The series of sulfate and organics by AMS correlated well ($R^2 = 0.76$ for sulfate, $R^2 = 0.74$ for organics) with the results measured by SPAMS, seen in Fig. 2a. However, poor correlations ($R^2 = 0.32$ for NH_4^+, $R^2 = 0.74$ for NO_3^-) were present for the series of NH_4^+ and NO_3^- detected by the SPAMS and AMS. It means that the detection for aerosol specie of NH_4^+, NO_3^- and Cl^- would be lost by SPAMS or AMS. This can also be verified by the signal intensity of ion mass spectra. Intense peaks of K^+, Na^+, C_n^+ and CO_2^+ with weak $C_nH_m^+$ were present in the positive spectrum of SPAMS detection. While extremely weak signal of NH_4^+ was present in the positive spectrum. High peaks of HSO_4^-, NO_3^- and NO_2^- with weak peak of Cl^- were appeared in the negative spectrum. Contrarily, strong peaks of NH_4^+ with weak intense peaks of NO_3^- and few peaks of Cl^- were present in the spectrum of AMS.

Correlation analyses were used to evaluate the relationships between aerosol species. A significant positive correlation ($r = 0.902$ for AMS and $r = 0.938$ for SPAMS, $p < 0.01$) between SO_4^{2-} and Cl^- was observed, suggesting that SO_4^{2-} and Cl^- may have the same sources. The species of SO_4^{2-} and Cl^- in the ambient aerosols can be from marine sources or fossil combustion (especially coal combustion). Generally, coarse particles were mainly from sea salt, while fine particles were mainly from coal combustion. As seen in Fig. 1a, the wind

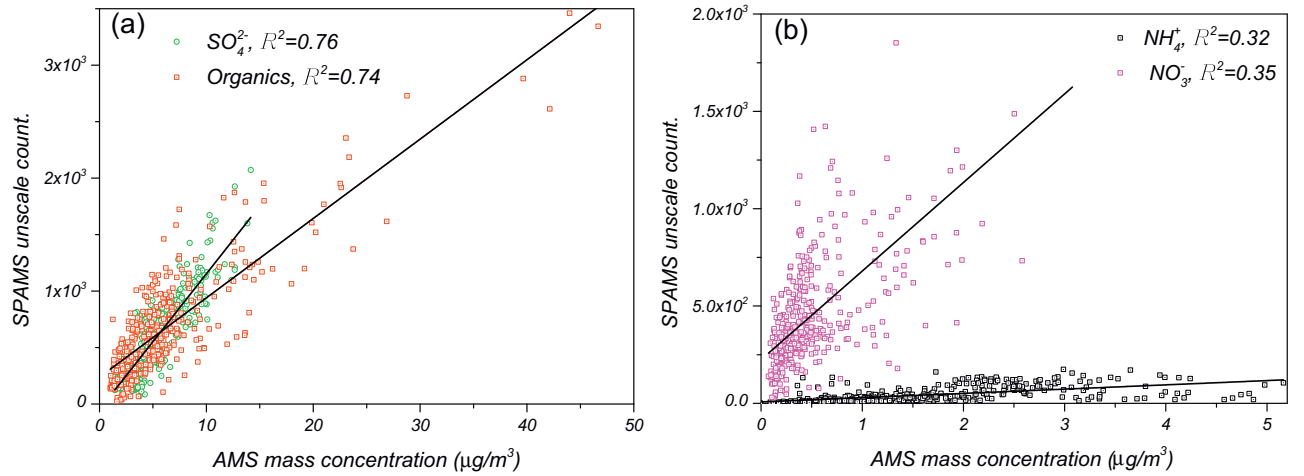

Fig. 2 – Correlation of AMS mass concentration and SPAMS particle number count during the whole observation period. (a) SO_4^{2-} and organics; (b) NH_4^+ and NO_3^-.

direction during the observation period was mainly northwest and northeast. The air masses were from manufacturing districts. As seen in Fig. 3, most of the particles were in small size in this study. According to the air mass transportation and particle size distribution, the major source of SO_4^{2-} and Cl^- was probably from coal combustion. However, as Xiamen was an island and the observation site was located at the seaside. That means sea salt also contributed to the source of SO_4^{2-} and Cl^- in this study. High correlation (r = 0.795, p < 0.01) was observed between SO_4^{2-} and NH_4^+ by AMS, while low correlation (r = 0.389, p < 0.01) was present between SO_4^{2-} and NH_4^+ by SPAMS. Additionally, the correlations between NH_4^+ and other

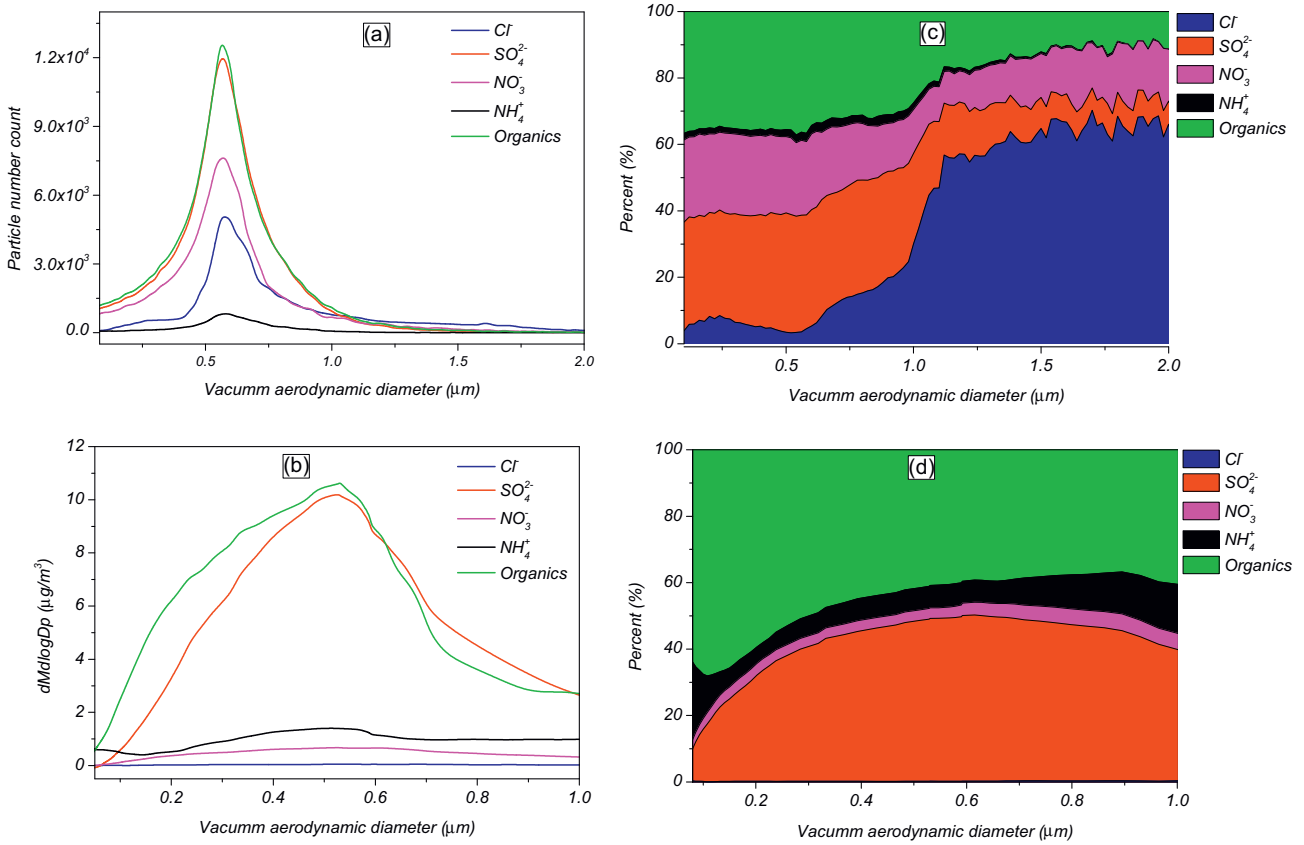

Fig. 3 – Average chemically speciated size distributions and size-resolved percent fraction of chemical compositions measured by AMS and SPAMS. (a) Particle size distribution by SPAMS, (b) percent fraction by SPAMS, (c) particle size distribution by AMS, (d) percent fraction by AMS.

species by SPAMS were weaker than the values given by the AMS, indicating that the detection of NH_4^+ would be lost by SPAMS. Generally, SO_4^{2-} and NO_3^- were believed to be the secondary aerosol species and in good correlation between each other (Wang et al., 2006). Significant positive correlation was identified between SO_4^{2-} and NO_3^- ($r = 0.676$, $p < 0.01$) with SPAMS measurement, however, weak correlation between SO_4^{2-} and NO_3^- ($r = 0.233$, $p < 0.01$) was present with AMS measurement. It is useful to find that the correlations between NO_3^- and other species (except NH_4^+) obtained by the SPAMS were better than the results given by AMS. The same phenomena of Cl^- were observed in this study. The correlations between Cl^- and other species by AMS were weaker than those by SPAMS (except NH_4^+).

2.3. Influence of particle size in detection

Note that the effective particle size range was 0.2–2.5 μm for SPAMS detection, while it was from 0.01 to 1.0 μm for AMS measurement. Hence, the discrepancy in measurement particle size range of two instruments would also affect measuring results of aerosol concentration. To clarify the influence of measurement particle size range on the measurement results, Fig. 3 illustrates the average chemically speciated size distributions and size-resolved fraction of chemical compositions measured by AMS and SPAMS. A unimodal distribution with a major accumulation mode peaking at a vacuum aerodynamic diameter of 550 nm was present with SPAMS, seen in Fig. 3a. Most of the particles were in the size range of 0.2–1.0 μm, accounting for over 98% of the total particles. A similar size distribution of aerosol species was present with AMS measuring, peaking at 545 nm (seen in Fig. 3c). Particles in the size range of 0.2–1.0 μm accounted for more than 97% of the total particles. That means majority particles were in the size range of 0.2–1.0 μm in this study, which was the same size range for both instruments measuring. In other words, most of aerosol particles (over 97%) can be detected by both AMS and SPAMS. Hence, the differences of measuring results were not determined by the discrepancy in measurement particle size range of AMS and SPAMS. Since particles with diameter larger than 1 μm or smaller than 0.2 μm only accounted for less than 3%, the influence of those particles on the measurement results were negligible in this case.

2.4. Factors affecting the detection results of aerosol species by AMS and SPAMS

2.4.1. Detection of NH_4^+ species

As mentioned above, extremely low particle number count of NH_4^+ was given by SPAMS. Previous studies have found that there was a great difference of the NH_4^+ particle number count measured by SPAMS, comparing to the mass concentration detected by other methods (Fu et al., 2014). This may be caused by the relative low ion signal intensity of NH_4^+ comparing to the high signal intensity of SO_4^{2-} and NO_3^-. In this case, NH_4^+ signal was ignored and resulted in low NH_4^+ particle count. However, it may be not the primary reason for low NH_4^+ particle number count with SPAMS measurement in this study. Note that a laser with wave length of 266 nm was used to ionize the particles in SPAMS detection. The Nd:YAG laser used in the instrument could not ionize the $(NH_4)_2SO_4$ crystal. In this case, if $(NH_4)_2SO_4$ was the main form of ammonium in aerosols, NH_4^+ and SO_4^{2-} could not be detected by SPAMS effectively. However, $(NH_4)_2SO_4$ can be volatilized when the temperature was higher than 300°C. Hence, the NH_4^+ can be detected effectively by AMS, since thermal volatilization was used in this instrument. Low number count of NH_4^+ with SPAMS detection but high NH_4^+ concentration with AMS measurement results suggested that the detection of NH_4^+ by SPAMS would be lost if the NH_4^+ was in the form of $(NH_4)_2SO_4$.

In order to substantiate that low NH_4^+ particle number count obtained by SPAMS was caused by the detection loss, the existence form of ammonia in ambient aerosols should be confirmed. It is the fact that vapor pressure of ammonium nitrate is much higher than ammonium sulfate, NH_4NO_3 can be favorable formed only when sufficiency of NH_3 and high humidity were present in the atmosphere (Calvert et al., 1978; Stelson and Seinfeld, 1982). The mole ratio of $[NH_4^+]/[SO_4^{2-}]$ was used to substantiate the form of ammonium. As mentioned above, NH_4^+ and SO_4^{2-} can be detected efficiently by AMS, the data of NH_4^+ and SO_4^{2-} concentration can be used to describe the ammonium in ambient aerosol (Cross et al., 2007). As seen in Fig. 4, most of the average mole ratio of $[NH_4^+]/[SO_4^{2-}]$ in aerosol particles was lower than 2 during the observation period, suggesting that $(NH_4)_2SO_4$ was the main form of ammonium in aerosols in this study. When the dots were over the line of $y = 2x$ only, the NH_4^+ was sufficient to neutralize the SO_4^{2-} and the NH_4NO_3 could be formed. In order to further demonstrate the above result, the value of mole ratio of $[NH_4^+]/[SO_4^{2-}]$ was also given using ICs detection. All of the dots given by ICs measurement were below the line of $y = 2x$ in this study. As mentioned above, $(NH_4)_2SO_4$ cannot be detected effectively using SPAMS. It was the reason that the concentration of ammonium measured by SPAMS was extremely low in this study. It is the case that SO_4^{2-} was also underestimated, which can be confirmed by the relative contribution of SO_4^{2-} during the observation period. As seen in Fig. 1b, c, the percentage of SO_4^{2-} measured by SPAMS was lower than the value given by AMS. However, if the NH_4^+ was in the form of other ammonium compounds, NH_4^+ would be detected by SPAMS effectively. High particle number count

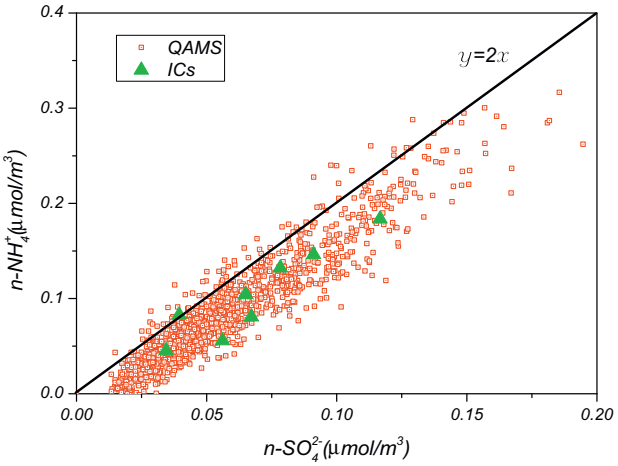

Fig. 4 – Scatter plot of n-SO_4^{2-} *vs.* n-NH_4^+.

of NH_4^+ can also be present with SPAMS measurement. But in this study low particle number count of NH_4^+ with SPAMS measurement was caused by the ineffective detection of $(NH_4)_2SO_4$.

2.4.2. Detection of NO_3^- and Cl^- species

As seen in Fig. 1, high value of Cl^- and NO_3^- particle number counts was detected by SPAMS, while extremely low concentrations of Cl^- and NO_3^- were measured by the AMS. The detection loss of Cl^- and NO_3^- species by AMS or over-valuation of Cl^- and NO_3^- species with SPAMS detection could contribute to the result in this study. To clarify the influence of different instruments on the detection of aerosol species, three instruments including ICs, AMS and SPAMS were used simultaneously to measure the aerosol species of NH_4^+, SO_4^{2-}, Cl^- and NO_3^- in this study. The mass concentration of aerosol species in the previous studies over Xiamen and the average concentration of aerosol species of NH_4^+, SO_4^{2-}, Cl^- and NO_3^- measured by AMS, ICs and SPAMS are illustrated in Table 1. The mean mass concentration of NH_4^+ measured by ICs was 1.86 ± 0.50 μg/m^3 and similar with the AMS measurement of 1.75 ± 0.60 μg/m^3, which was lower than the previous studies (3.24 μg/m^3 obtained by Liu et al. (2015) and 3.62 μg/m^3 obtained by Zhang et al. (2012)). However, extremely low particle number count of NH_4^+ particle was present with SPAMS. It confirmed that the detection loss of NH_4^+ by SPAMS occurred in this study, which can be further demonstrated by the relative contribution of particle species. NH_4^+ accounted for 13.96%, 20.33% and 2.67% individually for ICs, AMS and SPAMS measurement.

Contrarily, the average mass concentration of Cl^- and NO_3^- measured by AMS was 0.06 ± 0.11 μg/m^3 and 0.66 ± 0.36 μg/m^3, which was much lower than the value (3.25 ± 0.42 μg/m^3 for NO_3^- and 2.99 ± 0.46 μg/m^3 for Cl^-) given by ICs in this study and also lower than the previous studies (Liu et al., 2015; Zhang et al., 2012). That means that the mass concentration of Cl^- and NO_3^- measured by AMS was underestimated in this case. However, high particle number count of NO_3^- and Cl^- was obtained by SPAMS, accounting for 32.55% and 22.54% individually, which was similar with the results (25.96% for NO_3^- and 11.36% for Cl^-) given by ICs, but much higher than the value (6.56% for NO_3^- and 0.51% for Cl^-) obtained by AMS. Note that AMS could only detect the resolved composition of volatile and semi-volatile PM. The oven temperature used in the experiment was about 680°C. When the melting point of chemical composition was higher than the oven temperature, these refractory particles could not be resolved. Hence, detections of those species were lost. In this case, sea salt is not flash evaporating on the AMS heater and can therefore not be detected with the same efficiency as other species. Previous studies have found that sea salt particles from sea water were one of the important compositions in the atmosphere of Xiamen and sea salt were the main form of chloride in aerosols (Yan et al., 2013), suggesting that the detection of Cl^- would be lost mostly in this study and resulting in an extremely low mass concentration of Cl^- by AMS. Contrarily, most of the nitrates were not refractory compounds, which can be volatilized with the oven temperature. As mentioned above, most of NH_4^+ was in the form of $(NH_4)_2SO_4$, indicating that the bulk NO_3^- species may be in the form of $NaNO_3$, KNO_3 *etc.* Note that these nitrates can decompose into gaseous products (N_2) easily in high temperature, which would affect the NO_3^- species detection of AMS. Hence the detection of NO_3^- species was partly lost with AMS measurement.

Relative contribution of NO_3^- and Cl^- given by SPAMS was higher than the value given by ICs analysis. As mentioned above, over-valuation of NO_3^- and Cl^- concentrations by SPAMS can also contribute to the high value of Cl^- and NO_3^- relative percentages in this study. Note that *m/z* 35 [Cl^-] and *m/z* 36 [HCl^+] were used to identify the Cl^- for SPAMS and AMS detection respectively, which was the unique fragment ion for both instruments. That means that no other ions would be recognized as Cl^-, indicating that over-valuation of Cl^- species by SPAMS could not be occurred in this case. The fragment ions of NO_3^- were *m/z* 30 [NO^+], *m/z* 46 [NO_2^+] and *m/z* 63 [HNO_3^+] with AMS analysis, while *m/z* 46 [NO_2^-] and *m/z* 62 [NO_3^-] were the special fragment ions with SPAMS detection. Intense peaks of *m/z* 46 [NO_2^-] and *m/z* 62 [NO_3^-] were present simultaneously in the negative spectrum, hence, NO_3^- species can be well identified by SPAMS. In this case, other ions could be eliminated from the NO_3^- species with SPAMS measurement.

2.4.3. Detection of SO_4^{2-} and organics

High concentration of SO_4^{2-} was present by three instruments, indicating that the SO_4^{2-} can be efficiently detected by three instruments. In this study, *m/z* 48 [SO^+], *m/z* 64 [SO_2^+], *m/z* 80 [SO_3^+], *m/z* 81 [HSO_3^+] and *m/z* 98 [$H_2SO_4^+$] were used to characterize the sulfate with AMS measurement, and *m/z* 80 [SO_3^-] and *m/z* 97 [HSO_4^-] were the special fragment ions of sulfate for SPAMS. Therefore, sulfate can be well identified for both instruments. However, the detection of organics was

Table 1 – Aerosol species concentration investigated in previous studies and detected by different instruments during the whole observation period in this study.

Time	Aerosol species				Reference
	NO_3^-	SO_4^{2-}	NH_4^+	Cl^-	
Summer 2005	0.6	6.8	2.7	0.8	(Zhaung, 2007) (μg/m^3)
Sep 2009	4.32	9.85	3.62	0.77	(Zhang et al., 2012) (μg/m^3)
Autumn 2013	3.27	6.57	3.24	0.21	(Liu et al., 2015) (μg/m^3)
2013.09.12–20	3.25 ± 0.42	6.12 ± 2.03	1.86 ± 0.50	1.29 ± 0.46	ICs (This study) (μg/m^3)
2013.09.12–20	0.66 ± 0.36	6.07 ± 2.23	1.75 ± 0.60	0.06 ± 0.11	AMS (This study) (μg/m^3)
2013.09.12–20	488 ± 186	633 ± 198	40 ± 15	338 ± 107	SPAMS (This study) (Number Count.)

ICs: ion chromatography system; AMS: Aerodyne Aerosol Mass Spectrometer; SPAMS: Single Particle Aerosol Mass Spectrometer.

more complex, comparing to the other species. Hydrocarbon (C_nH_m) and oxygenated ($C_nH_mO_y$) organic aerosols were given by AMS with fragment ions of CO_2^+, HCO^+, $H_3C_2O^+$, and $C_xH_y^+$. Similar ion fragments of $C_xH_yO_z^+$, $C_xH_yO_z^-$, $C_xH_y^+$ and $C_xH_y^-$ were used to classify the organic species for SPAMS detection.

2.5. *Organic pollutants analysis*

A pollution event (event 2) was present with a dramatical increase of organic concentration which accounted for more than 50% and 75% of the total particles with SPAMS and AMS measurement, as seen in Fig. 1. The pollution event was caused by the organics in this study. It is useful to determine the pollutant sources by classifying the organics into different types. For AMS analysis, the total concentration of organics was given by the sum of the signal of all *m/z*'s organic spectra. That means organic spectra can be quantitative and decomposed into a linear combination of individual organic species with spectra. In this study, the mass spectra of organic aerosol was classified into two types, hydrocarbon-like organic aerosol (HOA) and oxygenated organic aerosol (OOA), using Positive Matrix Factorization (PMF, Pattero and Tapper, 1994). Taken together the two factors accounted for 97.6% of the measured organic mass (Yan et al., 2015). As seen in Fig. 5a and c, the HOA MS revealed ion series characteristic of long chain hydrocarbons (C_mH_n such as *m/z* 27, *m/z* 43, *m/z* 57, and *m/z* 71), which was regarded as the representation of the spectrum of fresh fossil fuel exhaust aerosol. During event 2, the HOA MS was more complicated with high fraction of the total organics, especially the increase of macromolecular hydrocarbons. The OOA MS represented the characteristic features of oxidized organic material, such as a major peak at *m/z* 44 (CO_2^+). In this study, the OOA components during event 2 showed little different from those during event 1, seen in Fig. 5b and d.

Generally, OOA was intensely correlated and mixed with the secondary species, such as NO_3^-. SO_4^{2-} and NH_4^+, suggesting that OOA was associated with the secondary organic aerosol (SOA). High concentration of OOA represented that serious SOA pollutants appeared in the ambient atmosphere. HOA was highly correlated with element carbon, CO and NO, which was classified as the primary emissions. High mass concentration of HOA was present during event 2, accounting for 73% (±22.5%) to the total organic mass concentration, seen in Fig. 7. However, this value was about 45% (±21.2%) during event 1. That means that pollutants during event 2 were determined by the increase of HOA, associating with the primary organic aerosol (POA). According to the change of the major wind direction during event 2, seen in Fig. 1a, the pollution event was caused by the primary emission from the manufacturing districts located to the northwest of the sampling site. This can be further confirmed by the SPAMS measurement.

To identify the organic composition of aerosol particles measured by SPAMS, the organic particles were classified into two major subtypes: POA and SOA in this study, which were yielded using ART-2a algorithm based on the positive and negative mass spectra of organic particles. The average positive and negative mass spectra of the two classes are shown in Fig. 6.

POA was regarded as to direct emission aerosols with few conversions in the ambient atmosphere, which was rich in element carbon and hydrocarbons. As seen in Fig. 6a, Strong peaks of K^+ and the progressions of $C_nH_m^+$ (such as *m/z* 27 $C_2H_3^+$, *m/z* 43 $C_3H_7^+$, *m/z* 51 $C_4H_3^+$, *m/z* 63 $C_5H_3^+$, and *m/z* 79 $C_6H_7^+$) were present in the positive spectrum. Hydrocarbon fragment ions with SPAMS measurement were similar with the measurement results of HOA given by AMS, seen in Fig. 5a. In the negative spectrum, POA particles were dominated by C_n^-, CHO_2^- and CN^- with weak peaks of $C_nH_m^-$ and NO_3^-. Comparing with the mass spectra during the pollution period, the types of hydrocarbons were less in the positive spectrum. But the negative spectrum of POA showed little discrepancy between event 1 and event 2. SOA was typically generated by gas to particle reactions in the ambient atmosphere, correlating well with those secondary species. In this study, intense peaks of K^+, Na^+ and CO_2^+ were present in the positive spectrum of SOA, seen in Fig. 6b while the negative spectrum of SOA particles was abundance of secondary species of NO_2^-, NO_3^- and HSO_4^- with O^-, OH^-, and $C_2H_3O^-$. High correlation (R^2 = 0.93) between SOA and the secondary inorganic species was observed in this study. It is useful to find that the average SOA spectra during

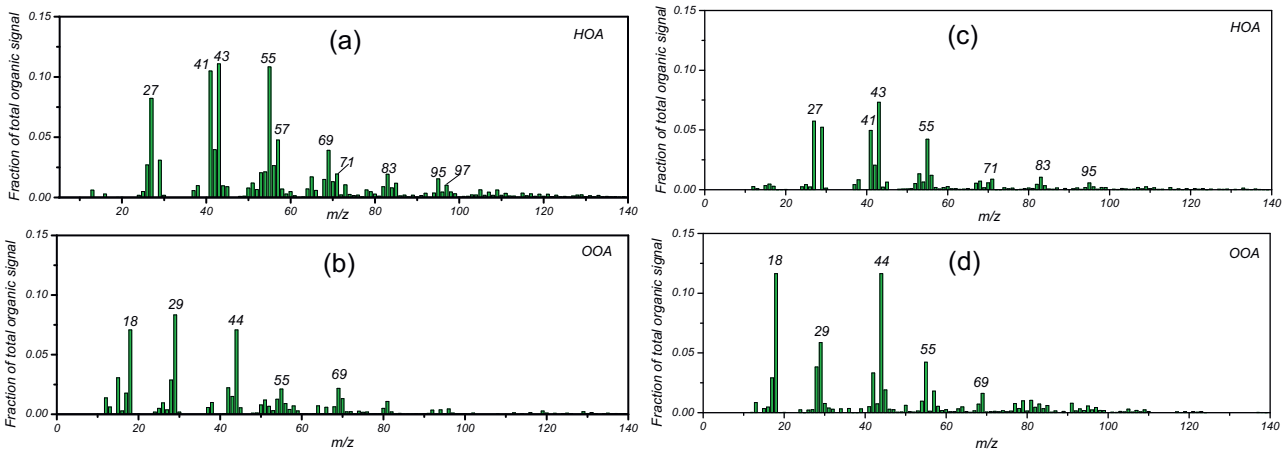

Fig. 5 – Average mass spectra of organic aerosol clusters given by AMS measurement. (a) HOA during event 2, (b) OOA during event 2, (c) HOA during event 1, (d) OOA during event 1.

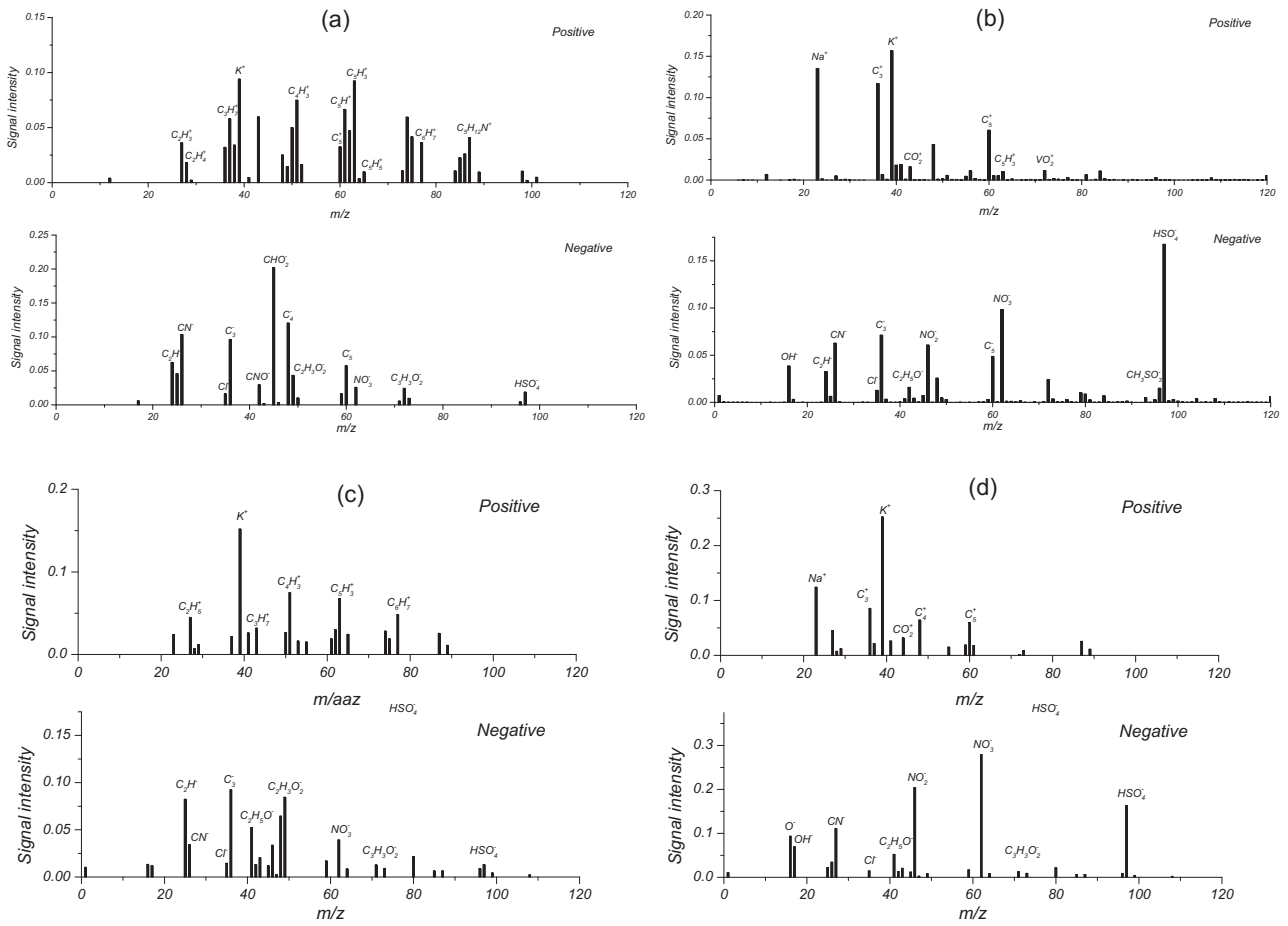

Fig. 6 – Average mass spectra of organic aerosol clusters given by SPAMS detection, (a) POA during event 2, (b) SOA during event 2, (c) POA during event 1, (d) SOA during event 1.

event 1 were similar with the spectra during event 2. That means that the formation of SOA did not change during the pollution period. Therefore, the pollutants during event 2 were dominated by the primary organic emission. As seen in Fig. 7, POA accounted for 30% (±18.6%) of the total particles during event 1, while this value increased to 65% (±25.1%) during event 2. Note that the variations of POA and SOA obtained from SPAMS during event 1 and event 2 were in accordance with the analysis of HOA and OOA given by the measurement results of AMS. Hence, organic pollutant sources can be well identified with both instruments.

2.6. Inorganic pollutants analysis

2.6.1. Analysis of aerosol sources

Generally, the particle source analysis was carried out based on the particle mass concentration. Such as, the mass ratio of NO_3^-/SO_4^{2-} in airborne aerosols was used to evaluate the relative importance of stationary sources *versus* mobile sources (Gao et al., 2009). High value of NO_3^-/SO_4^{2-} ratio occurred when the influence of motor vehicle emission exceeded those from coal combustion (Arimoto et al., 1996; Du et al., 2011). Fig. 8a illustrates the correlation of NO_3^- and SO_4^{2-} mass concentration measured by AMS and ICs during the whole observation period. The mean value of NO_3^-/SO_4^{2-} given by AMS was about 0.11, which was much lower than the value of 0.43 given by ICs, which was similar with previous studies (0.49 during autumn 2013) in Xiamen (Liu et al., 2015) and about 0.44 during September 2009 in Xiamen (Zhang et al., 2012). However, the ratio of NO_3^-/SO_4^{2-} given by AMS was much lower in this study, suggesting that stationary sources (coal combustion) were the

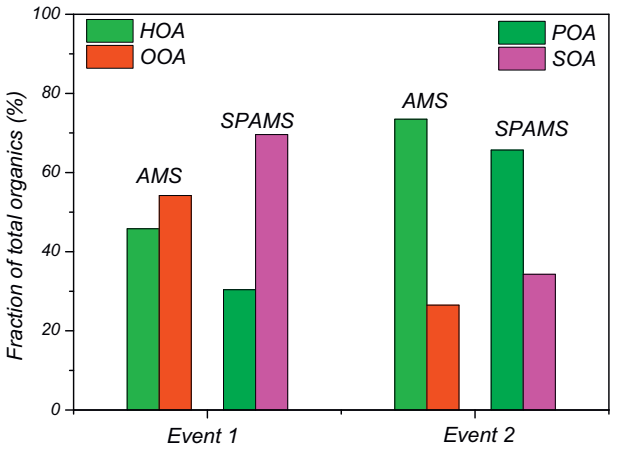

Fig. 7 – Fraction of different clusters of total organics obtained by AMS and SPAMS.

dominant sources of pollutants in Xiamen. Note that emissions from stationary sources and mobile sources would be relative constant in a long period. In this case, when the value of NO_3^-/SO_4^{2-} given by AMS was used to evaluate the influence of stationary sources *versus* mobile sources, the importance of stationary sources would be overestimated.

Since SPAMS could only provide the particle number count, the ratio of NO_3^-/SO_4^{2-} cannot be calculated by the mass concentration. In this study, we used the particle number count to calculate the value of NO_3^-/SO_4^{2-}. As seen in Fig. 8b, the mean ratio of NO_3^-/SO_4^{2-} calculated by SPAMS was about 0.52, which was higher than the value 0.44 given by ICs. But it was close to the previous investigation (0.49 during autumn 2013) in Xiamen (Liu et al., 2015).

2.6.2. Characteristic of aerosol acidity

Aerosol acidity is very important as it has a significant concern with the hygroscopic growth, heterogeneous condensational enlargement, toxicity and multiphase reactions. The acidity of aerosol was determined by comparing the NH_4^+ mass concentration measured by the instrument to the amount needed to fully neutralize the anions measured (Sun et al., 2010):

$$NH_{4\,predict}^{+} = 18x(2xSO_4^{2-}/96 + NO_3^-/62 + C1^-/35.5) \quad (1)$$

where the SO_4^{2-}, NO_3^- and Cl^- represent the mass concentrations ($\mu g/m^3$) of the species; the denominators correspond to their molecular weights. Aerosols were considered as more acidic while the measured NH_4^+ concentration was lower than predicted NH_4^+ and as bulk neutralized if the measured NH_4^+ concentration was similar with the predicted value. Fig. 9 shows the scatter plot of measurement and prediction NH_4^+ obtained by ICs and AMS. The correlation between measurement and prediction NH_4^+ was very tight (R^2 = 0.87 for ICs and R^2 = 0.88 for AMS), with a slope of 0.56 and 0.81 during the whole observation period. As mentioned about, NH_4^+ was detected efficiently by AMS while the detection of Cl^- and NO_3^- were partly lost, resulting in the underestimate of predicted NH_4^+. The slope of the correlation between measurement and prediction NH_4^+ with AMS measurement was more closed to 1, showing that aerosols were more bulk neutralized when using the data to analyze the aerosol acidity. Hence, there was a deviation when those measurement results obtained from AMS were used to analyze the ambient aerosol acidity. However, good correlation between measured and predicted NH_4^+ was present for ICs detection and the slope was lower than the value given by AMS, indicating that the result given by ICs would better represent the actual aerosol acidity, as Cl^- and NO_3^- species were well quantified by ICs in this study.

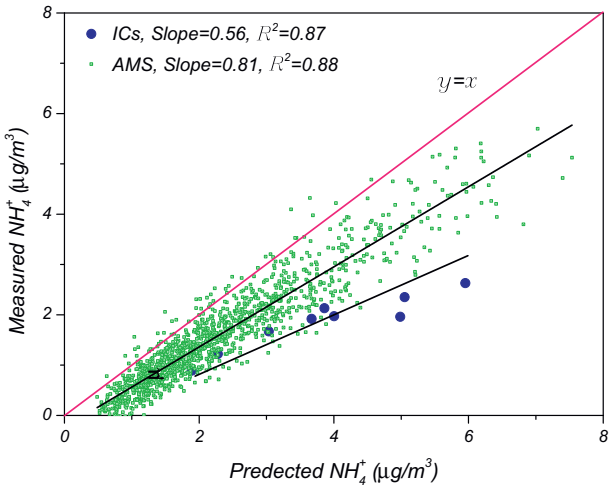

Fig. 9 – Scatter plot that compares predicted NH_4^+ *vs.* measured NH_4^+ obtained by ICs and AMS.

3. Conclusions

Chemical compositions and size distribution were obtained from 9th to 21st September using two different types of aerosol mass spectrometers AMS and SPAMS in Xiamen, representing the coastal urban area. Five obvious processes were classified during the whole observation period, according to variations of the

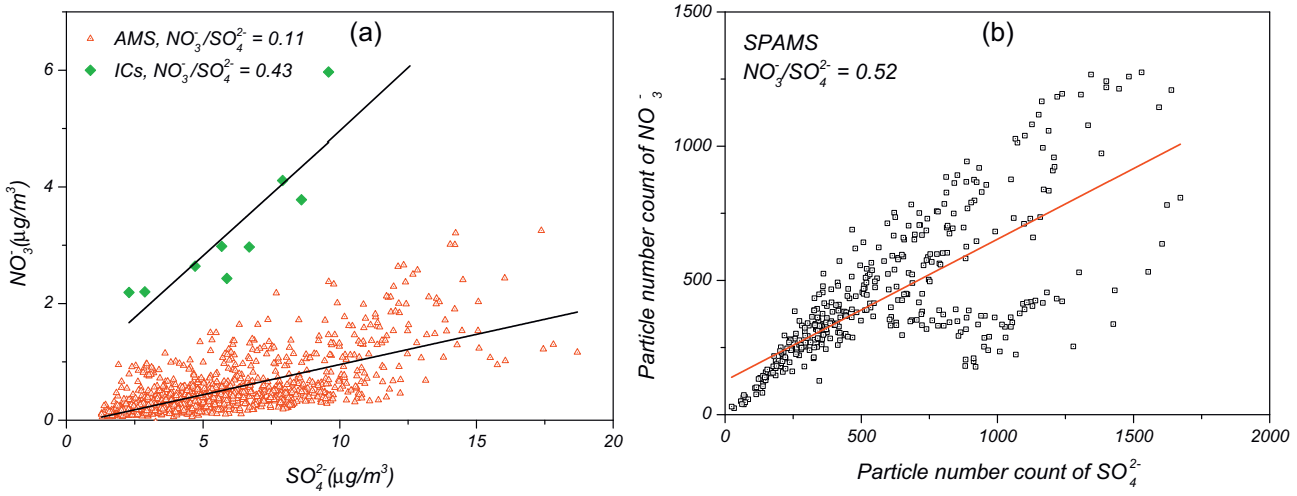

Fig. 8 – Correlation of NO_3^- and SO_4^{2-} measured by different instruments, (a) AMS and ICs, (b) SPAMS.

aerosol properties and meteorological parameters. The aerosol chemical compositions during event 1, event 3 and event 5 were very similar. Organics and sulfate were the dominant aerosol components and the organic concentration was higher than sulfate, representing the general aerosol pollutant properties over Xiamen. Organics were the only dominant aerosol component in the aerosol particles during event 2. High mass concentration of HOA was present during event 2, accounting for 73% (±22.5%) to the total organics mass concentration, indicating that the pollution event was caused by the primary emission from the manufacturing districts located to the northwest of the sampling site.

A similar significant accumulation mode with a peak size of 540–550 nm was observed during the whole period for both AMS and SPAMS. Most of the particles were in the size range of 0.2–1.0 μm, accounting for over 97% of total particles. Similar trend with the changes of time series measured by SPAMS and AMS were present, indicating that both instruments can well identify the characteristics of atmospheric aerosols. Organics, as well as sulfate, measured by AMS correlated well with the value given by SPAMS. However, high particle number count of Cl^- and NO_3^- particles was detected by SPAMS, while the concentration of Cl^- and NO_3^- was extremely low with AMS measurement. Contrarily, high value of NH_4^+ was measured by AMS, while very low particle number count of NH_4^+ was detected by SPAMS. The detection of NH_4^+ was lost by SPAMS due to the inefficient measurement of $(NH_4)_2SO_4$ which was the major form of ammonium in this study, resulting in an extremely low NH_4^+ concentration. However, the measurement of Cl^- was lost by AMS because of inefficient detection of the refractory particles.

Both of AMS and SPAMS can well identify the organic clusters of aerosol particles. The variations of POA and SOA obtained from SPAMS during event 1 and event 2 were in accordance with the analysis of HOA and OOA given by the measurement results of AMS. However, overestimate or underestimate of the aerosol properties was present in some circumstances because of the detection loss of some species for both instruments.

Acknowledgments

This study is supported by the Natural Science Foundation of Fujian Province, China (No. 2015J05024), financially supported by Qingdao National Laboratory for marine science and technology (No. QNLM2016ORP0109), the National Natural Science Foundation of China (No. 21106018, No. 41305133), the Scientific Research Foundation of Third Institute of Oceanography, SOA (No. 2014027), the Special Fund for Marine Researches in the Public Interest (No. 2004DIB5J178). The authors gratefully acknowledge Guangzhou Hexin Analytical Instrument Company Limited for the SPAMS data analysis software.

Appendix A. Supplementary data

Supplementary data to this article can be found online at http://dx.doi.org/10.1016/j.jes.2017.06.030.

REFERENCES

Alfarra, M.R., Coe, H., Allan, J.D., Bower, K.N., Boudries, H., Canagaratna, M.R., et al., 2004. Characterization of urban and rural organic particulate in the lower fraser valley using two aerodyne aerosol mass spectrometers. Atmos. Environ. 38, 5745–5758.

Allan, J.D., Alfarra, M.R., Bower, K.N., Williams, P.I., Gallagher, M.W., Jimenez, J.L., et al., 2003. Quantitative sampling using an aerodyne aerosol mass spectrometer. Part 2: measurements of fine particulate chemical composition in two UK cities. J. Geophys. Res. 108, 4091.

Allen, J.O., 2005. YAADA: Software Toolkit to Analyze Single-particle Mass Spectral Data.

Aller, J.Y., Kuznetsova, M.R., Jahns, C.J., Kemp, P.F., 2005. The sea surface microlayer as a source of viral and bacterial enrichment in marine aerosols. J. Aerosol Sci. 36, 801–812.

Arimoto, R., Duce, R.A., Savoie, D.L., Prospero, J.M., Talbot, R., Cullen, J.D., et al., 1996. Relationships among aerosol constituents from Asia and the North Pacific during PEM-West. J. Geophys. Res. 101, 2011–2023.

Brook, R.D., Brook, J.R., Vincent, R., Rajagopalan, S., Silverman, F., 2002. Inhalation of fine particulate air pollution and ozone causes acute arterial vasoconstriction in healthy adults. Circulation 105, 1534–1536.

Buonanno, G., Stabile, L., Morawska, L., Russi, A., 2013. Children exposure assessment to ultrafine particles and black carbon: the role of transport and cooking activities. Atmos. Environ. 79, 53–58.

Calvert, J.G., Su, F., Bottenheim, J.W., 1978. Mechanism of the homogeneous oxidation of sulfur dioxide in the troposphere. Atmos. Environ. 12, 199–210.

Chalbot, M.C., Mcelroy, B., Kavouras, I., 2013. Sources, trends and regional impacts of fine particulate matter in southern Mississippi Valley: significance of emissions from sources in the Gulf of Mexico coast. Atmos. Chem. Phys. 13 (7), 3721–3732.

Cross, E.S., Slowik, J.G., Davidovits, P., Allen, J.D., Worsnop, D.R., Jayne, J.T., et al., 2007. Laboratory and ambient particle density determinations using light scattering in conjunction with aerosol mass spectrometry. Aerosol Sci. Technol. 41, 343–359.

Dall'Osto, M., Harrison, R.M., 2006. Chemical characterization of single airbone particles in Athens (Greece) by ATOFMS. Atmos. Environ. 40, 7614–7631.

Dall'Osto, M., Harrison, R.M., 2012. Urban organic aerosols measured by single particle mass spectrometry in the mega-city of London. Atmos. Chem. Phys. 12, 4127–4142.

Després, V.R., Huffman, A., Burrows, S.M., Hoose, C., Safatov, A.S., Buryak, G., 2012. Primary biological aerosol particles in the atmosphere: a review. Tellus Ser. B 64, 15598.

Drewnick, F., Schwab, J.J., Jayne, J.T., Canagaratna, M., Worsnop, D.R., Demerjian, K.L., 2004. Measurement of ambient aerosol composition during the PMTACS-NY 2001 using an aerosol mass spectrometer part I: mass concentrations. Aerosol Sci. Technol. 38, 92–103.

Du, H.H., Kong, L.D., Cheng, T.T., Chen, J.M., Du, J.F., Li, L., et al., 2011. Insights into summertime haze pollution events over Shanghai based online water-soluble ionic composition of aerosols. Atmos. Environ. 45, 5131–5137.

Falkowska, L., Lewandowska, A., 2004. Sulphates in particles of different sizes in the marine boundary layer over the southern Baltic Sea. Oceanologia 46 (2), 201–215.

Fu, H., Yan, C., Zheng, M., Cai, J., Li, X., Zhang, Y., et al., 2014. Application of on-line single particle aerosol mass spectrometry (SPAMS) for studying major components in fine particulate matter. Environ. Sci. 35, 4070–4077.

Gao, J., Wang, T., Zhou, X.H., Wu, W.S., Wang, W.X., 2009. Measurement of aerosol number size distributions in the Yangtze River delta in China: formation and growth of particles under polluted conditions. Atmos. Environ. 43, 829–836.

Jayne, J.T., Leard, D.C., Zhang, X., Davidovits, P., Smith, K.A., Kolb, C.E., et al., 2000. Development of an aerosol mass spectrometer for size and composition analysis of submicron particles. Aerosol Sci. Technol. 33, 49–70.

Jimenez, J.L., Jayne, J.T., Shi, Q., Kolb, C.E., Worsnop, D.R., Yourshaw, I., et al., 2003. Ambient aerosol sampling with an aerosol mass spectrometer. J. Geophys. Res. 108, 8425.

Kanakidou, M., Seinfeld, J.H., Pandis, S.N., Barnes, I., Dentener, F.J., Facchini, M.C., et al., 2005. Organic aerosol and global climate modelling: a review. Atmos. Chem. Phys. 5, 1053–1123.

Kang, C.M., Lee, H.S., Kang, B.W., Lee, S.K., Sunwoo, Y., 2004. Chemical characteristics of acidic gas pollutants and $PM_{2.5}$ species during hazy episodes in Seoul, South Korea. Atmos. Environ. 38, 4749–4760.

Kim, K.W., Kim, Y.J., Bang, S.Y., 2008. Summer time haze characteristics of the urban atmosphere of Gwangju and the rural atmosphere of Anmyon, Korea. Environ. Monit. Assess. 141, 189–199.

Li, L., Huang, Z., Dong, J., Li, M., Gao, W., Nian, H., et al., 2011. Real time bipolar time-of-flight mass spectrometer for analyzing single aerosol particles. Int. J. Mass Spectrom. 303, 118–124.

Li, L., Li, M., Huang, Z.X., Gao, W., Nian, H.Q., Fu, Z., et al., 2014. Ambient particle characterization by single particle aerosol mass spectrometry in an urban area of Beijing. Atmos. Environ. 94, 323–331.

Liu, Y., Zhang, Y., Huang, S., Hu, Q., Lin, C., Wu, S.P., 2015. Size distribution of water soluble ions in aerosols from coastal urban and open sea. J. Xiamen Univ. Nat. Sci. 4, 531–539.

Ma, L., Li, M., Zhang, H., Li, L., Huang, Z., Gao, W., et al., 2016. Comparative analysis of chemical composition and sources of aerosol particles in urban Beijing during clear, hazy, and dusty days using single particle aerosol mass spectrometry. J. Clean. Prod. 112, 1319–1329.

O'Dowd, C.D., Facchini, M.C., Cavalli, F., Ceburnis, D., Mircea, M., Decesari, S., 2004. Biogenically driven organic contribution to marine aerosol. Nature 431, 676.

Pattero, P., Tapper, U., 1994. Positive matrix factorization: a non-negative factor model with optimal utilization of error estimates of data values. Environmetrics 5, 111–126.

Prather, K.A., 2009. Our current understanding of the impact of aerosols on climate change. ChemSusChem 2, 377–379.

Song, X.H., Hopke, P.K., Fergenson, D.P., Prather, K.A., 1999. Classification of single particles analyzed by ATOFMS using an artificial neural network, ART-2A. Anal. Chem. 71, 860–865.

Spencer, M.T., Shields, L.G., Prather, K.A., 2007. Simultaneous measurement of the effective density and chemical composition of ambient aerosol particles. Environ. Sci.Technol. 41, 1303–1309.

Stelson, A.W., Seinfeld, J.H., 1982. Relative humidity and temperature dependence of the ammonium nitrate dissociation constant. Atmos. Environ. 169, 83–92.

Steve, S., Mike, W., Ray, L., Rik, B., Manuel, D., Roy, M., 2012. Comparative study of single particle characterisation by transmission electron microscopy and time-of-flight aerosol mass spectrometry in the London. Atmos. Environ. 62, 400–407.

Sullivan, R.C., Guazzotti1, S.A., Sodeman, D.A., Prather, K.A., 2007. Direct observations of the atmospheric processing of Asian mineral dust. Atmos. Chem. Phys. 7, 1213–1236.

Sun, J.Y., Zhang, Q., Canagaratna, M.R., Zhang, Y.M., Ng, N.L., Sun, Y.L., et al., 2010. Highly time- and size-resolved characterization of submicron aerosol particles in Beijing using an aerodyne aerosol mass spectrometer. Atmos. Environ. 44, 131–140.

Wang, Y., Zhuang, G., Sun, Y., Zheng, A., 2006. The variation of characteristics and formation mechanisms of aerosols in dust, haze, and clear days in Beijing. Atmos. Environ. 40, 6579–6591.

Yan, J., Chen, l., Lin, Q., Zhao, S., Zhang, M., 2016. Effect of typhoon on atmospheric aerosol particle pollutants accumulation over Xiamen, China. Chemosphere 159, 244–255.

Yan, J., Chen, L., Lin, Q., Li, Z., Chen, H., Zhao, S., 2015. Chemical characteristics of submicron aerosol particles during a long-lasting haze episode in Xiamen, China. Atmos. Environ. 113, 118–126.

Yan, J., Chen, L., Lin, Q., Zhang, Y., Li, Z., 2013. A study of aerosol chemical compositions and size distribution property on the coastal area of southern Xiamen island. J. Appl. Oceanogr. 32, 455–460.

Yang, L., Bao, J., Yan, J., Liu, J., Song, S., Fan, F., 2010. Removal of fine particles in wet flue gas desulfurization system by heterogeneous condensation. Chem. Eng. J. 156 (1), 25–32.

Yin, L.Q., Niu, Z.C., Chen, X.Q., Chen, J.S., Xu, L.L., Zhang, F.W., 2012. Chemical compositions of $PM_{2.5}$ aerosol during haze periods in the mountainous city of Yong'an, China. J. Environ. Sci. 24, 1225–1233.

Zhang, Q., Jimenez, J.L., Canagaratna, M.R., Allan, J.D., Coe, H., Ulbrich, I., et al., 2007. Ubiquity and dominance of oxygenated species in organic aerosols in anthropogenically-influenced Northern Hemisphere mid latitudes. Geophys. Res. Lett. 34, L13801.

Zhang, F., Xu, L., Chen, J., Zhao, J., Yu, Y., Niu, Z., Yin, L., 2012. Chemical compositions and extinction coefficients of $PM_{2.5}$ in peri-urban of Xiamen, China, during June 2009–May 2010. Atmos. Res. 106, 150–158.

Zhang, F., Zhao, J., Chen, J., Xu, Y., Xu, L., 2011. Pollution characteristics of organic and elemental carbon in $PM_{2.5}$ in Xiamen, China. J. Environ. Sci. 23 (8), 1342–1349.

Zhao, J., Zhang, F., Xu, Y., Chen, J., 2011. Characterization of water-soluble inorganic ions in size-segregated aerosols in coastal city, Xiamen. Atmos. Res. 99, 546–562.

Zhaung, M., 2007. Research on chemical characteristics of Xiamen fine air particles. Mod. Sci. Instrum. 5, 113–115.